

# Physical factors affecting the transport and deposition of particles in saturated porous media

Xianze Cui, Quansheng Liu and Chengyuan Zhang

## ABSTRACT

Saturated sand box experiments were conducted to explore the effect of various physical factors on the transport and deposition of suspended particles in porous media. Red quartz powder and natural quartz sand were employed in the study and acted as suspended particles and porous media, respectively. Particles were injected into the sand box in two modes, i.e., pulse injection and continuous injection. Tests were performed at various particle concentrations, flow velocities, deposition rate coefficient and longitudinal dispersion coefficient by both injection modes. The breakthrough curves were described with the analytical solution of a convection–dispersion equation, in which first-order deposition kinetics were taken into account. Different behavior of suspended-particle transport and deposition in porous media was observed under different injection modes and experimental conditions. The results show that effluent concentration was approximately linear with the initial particle concentration. The deposition rate coefficient depends strongly on particle size and flow velocity, and the transport and deposition process was very sensitive to it. Furthermore, the longitudinal dispersion coefficient increases with increasing flow rate, and particles are easier to transport through pores as the longitudinal dispersion coefficient increases. This study shows the importance of particle concentration, flow velocity, deposition rate coefficient and longitudinal dispersion coefficient in the transport and deposition process of suspended particles.

**Key words** | deposition rate coefficient, flow velocity, longitudinal dispersion coefficient, particle concentration, sand box experiments

**Xianze Cui** (corresponding author)  
College of Hydraulic and Environmental  
Engineering,  
China Three Gorges University,  
No. 8, University Road,  
Yichang 443002,  
China  
E-mail: zexiancui1989@gmail.com

**Quansheng Liu**  
**Chengyuan Zhang**  
State Key Laboratory of Geomechanics and  
Geotechnical Engineering,  
Institute of Rock and Soil Mechanics, Chinese  
Academy of Sciences,  
Wuhan,  
China

## INTRODUCTION

Research on suspended particle transport and deposition in porous media is required to assess groundwater recharge efficiency and to protect drinking water supplies from contaminants (Sen 2011; Ward & Dillon 2012), to explore oil in low-permeability reservoirs and to microbially enhance oil recovery (Patel *et al.* 2015), to predict the stability of filter layers in the dam and to quantify colloid-facilitated transport of various contaminants (Rinck-Pfeiffer *et al.* 2000). Previous studies of particle transport, deposition and release mechanisms have mainly focused on colloids and microorganisms with sizes smaller than 1  $\mu\text{m}$  (Bradford & Torkzaban 2013),

and suspended particles with sizes larger than 5  $\mu\text{m}$  have only attracted significant attention recently (Wang *et al.* 2000; Kim & Lawler 2012; Liu *et al.* 2014, 2015).

For particles with a size larger than 10  $\mu\text{m}$ , hydrodynamic force, gravity and inertial effects are the dominant forces that control its fate (Kasel *et al.* 2013). For particles with smaller size (between 0.1 and 10  $\mu\text{m}$ ), factors such as electrostatic forces and Brownian motion can also contribute to particle deposition (Lanphere *et al.* 2014; Pugliese *et al.* 2015). The boundary between colloid and suspended particle is quite blurry, but it obeys the rule that as particle

size decreases, particle interactions become increasingly significant relative to external forces. Diverse correlations have been developed between experimental parameters (i.e. attachment coefficients, straining rate coefficients and detachment coefficient) and variables of physical, chemical and biological particles (Alvarez et al. 2007; Bedrikovetsky et al. 2011; Yuan et al. 2013).

Experimental and theoretical work has demonstrated that physical factors, such as particle concentration, flow velocity, deposition rate and longitudinal dispersion coefficient, may affect the transport and fate of suspended particles in saturated porous media (Ahfir et al. 2007, 2009; Bedrikovetsky et al. 2011). Published literature on this field was mainly focused on colloid particles with a size smaller than 10  $\mu\text{m}$ ; the transport and deposition mechanisms for bigger particles have not been systematically studied. In other words, the effects of these physical factors on the transport and deposition of suspended particles in natural porous media have not been studied thoroughly, especially in experiments. Therefore, a systematic study of the interactions between these factors is essential for understanding the process of suspended-particle transport and deposition in a saturated porous medium.

The objective of this work is to quantify the effects of particle concentration, flow velocity, deposition rate coefficient and longitudinal dispersion coefficient on the transport and deposition of suspended particles in a saturated porous medium. A series of experiments was conducted with a self-developed sand layer transportation-deposition testing system, and two injection modes, i.e., pulse injection and continuous injection, were adopted. The theoretical result of the convection-dispersion model fits the experimental data fairly well. In addition, the transport and deposition mechanisms of particles under various factors were investigated.

## THEORY

### Mathematical model

Under the conditions of steady-state and saturated flow, the transportation and deposition process of particles through porous media can be described with the convection-

dispersion equation, in which the deposition process is taken into account (Ahfir et al. 2007):

$$\frac{\partial C}{\partial t} = D_L \frac{\partial^2 C}{\partial x^2} - u \frac{\partial C}{\partial x} - K_{\text{dep}} C \quad (1)$$

where  $C$  is the particle concentration ( $\text{M}/\text{L}^3$ ),  $t$  is the time ( $\text{T}$ ),  $x$  is the travel distance of particles ( $\text{L}$ ),  $D_L$  is the longitudinal dispersion coefficient ( $\text{L}^2/\text{T}$ ),  $u$  is the average flow rate of water in the pores ( $\text{L}/\text{T}$ ),  $K_{\text{dep}}$  is the deposition rate coefficient ( $\text{T}^{-1}$ ).

It should be noted that the process of particle detachment is neglected in this equation.

Two modes of injection were studied in this work, i.e. pulse injection and continuous injection. The former way can describe instantaneous pollution in the stratum and the latter one can represent typical dispersal of pollution, as well as groundwater recharge with constant particle concentration.

For the way of pulse injection, the initial and boundary conditions are given by

$$\left. \begin{aligned} C(t=0, x) &= 0 \\ C(t, x=0) &= m/Q\delta(t) \\ C(t, x=\infty) &= 0 \end{aligned} \right\} \quad (2)$$

where  $m$  is the mass of injected particles ( $\text{M}$ ),  $\delta(t)$  is the Dirac delta function,  $Q$  is the flow rate ( $\text{L}^3/\text{T}$ ).

The analytical solution can be expressed as (Wang et al. 2000)

$$C(x, t) = \frac{mx}{Q\sqrt{4\pi D_L t^3}} \exp(-K_{\text{dep}} t) \exp\left[-\frac{(x-ut)^2}{4D_L t}\right] \quad (3)$$

For the way of continuous injection, the initial and boundary conditions are given by

$$\left. \begin{aligned} C(t=0, x) &= 0 \\ C(t, x=0) &= C_0 \\ C(t, x=\infty) &= 0 \end{aligned} \right\} \quad (4)$$

The analytical solution can be expressed as (Genuchten et al. 2013)

$$C(x, t) = \frac{C_0}{2} \exp\left[\frac{ux}{2D_L}(1-\phi)\right] \text{erfc}\left(\frac{x-ut\phi}{\sqrt{4D_L t}}\right) + \frac{C_0}{2} \exp\left[\frac{ux}{2D_L}(1+\phi)\right] \text{erfc}\left(\frac{x+ut\phi}{\sqrt{4D_L t}}\right) \quad (5)$$

with

$$\phi = \sqrt{1 + \frac{4K_{\text{dep}}D_L}{u^2}} \quad (6)$$

where  $\text{erfc}(x) = \frac{2}{\sqrt{\pi}} \int_x^\infty e^{-\eta^2} d\eta$  is the complementary error function.

For most applications of particle transport through porous media, the system is considered at steady state and the effect of hydrodynamic dispersion is always neglected (Tufenkji & Elimelech 2004). The deposition rate coefficient is assumed invariant (both spatially and temporally) under normal conditions. The relationship between retained particle concentration ( $S$ ) and particle concentration flow with water ( $C$ ) can be expressed as

$$\frac{\rho_b}{\phi} \frac{\partial S}{\partial t} = K_{\text{dep}} C \quad (7)$$

where  $\rho_b$  is the porous medium bulk density,  $\phi$  is porosity.

Thus we can obtain the solutions to Equations (1), (4) and (7) for continuous particle injection at concentration  $C_0$  and time period  $t_0$  (Tufenkji & Elimelech 2004):

$$S(x) = \frac{t_0 \phi K_{\text{dep}} C_0}{\rho_b} \exp\left[-\frac{K_{\text{dep}}}{v} x\right] \quad (8)$$

where  $v$  is the interstitial particle velocity.

Equation (8) is commonly referred to as the classical filtration model and has been widely used in describing the transportation of particles, colloids and microorganisms in saturated porous media (Lee et al. 2017).

### Sensitivity analysis of the model parameters

The transportation and deposition process of particles through porous media is affected by many parameters, thus it is of great importance to conduct a sensitivity analysis of the model parameters (Ouisse et al. 2012). In our study, parameters ( $D_L$ ,  $K_{\text{dep}}$ ,  $u$ ,  $m$ ) under pulse injection and parameters ( $D_L$ ,  $K_{\text{dep}}$ ,  $u$ ,  $C_0$ ) under continuous injection in the model were subjected to sensitivity analysis. The sensitivity analyses were conducted by fixing the remaining parameters and investigating the change trend

of particle concentration in the pores ( $C$ ) when a parameter changes. This procedure was conducted for  $D_L$ ,  $K_{\text{dep}}$ ,  $u$ ,  $m$  and  $C_0$ , separately, which may affect the process of particle transport and deposition. Referring to previous studies (Tufenkji & Elimelech 2004; Tufenkji 2007), the initial values of  $D_L$ ,  $K_{\text{dep}}$ ,  $u$ ,  $m$  and  $C_0$  were taken as  $4.1 \times 10^{-5} \text{ m}^2/\text{s}$ ,  $2 \times 10^{-2} \text{ 1/s}$ ,  $3 \times 10^{-3} \text{ m/s}$ ,  $5 \text{ g}$  and  $1.8 \times 10^{-5} \text{ m}^3/\text{s}$ , respectively. On this basis, particle concentration in the pores ( $C$ ) was calculated at  $x = 0.6 \text{ m}$  and  $t = 200 \text{ s}$  for continuous injection by making changes of  $\pm 10\%$ ,  $\pm 20\%$ ,  $\pm 30\%$ ,  $\pm 40\%$  and  $\pm 50\%$  on initial values of the four parameters. The peak concentration ( $C_p$ ) was calculated at  $x = 0.6 \text{ m}$  for pulse injection in the same way.

The relationship between peak concentration ( $C_p$ ) and the change of each parameter under pulse injection is shown in Figure 1. Under pulse injection mode, it can be seen that the change of peak concentration increases with the change of injected particle mass ( $m$ ) and flow rate ( $u$ ). The change of peak concentration ranges from  $-50\%$  to  $50\%$  for the change of injected particle mass and  $-95.6\%$  to  $394.2\%$  for the change of flow rate. Meanwhile, change of peak concentration decreases with the change of deposition rate ( $K_{\text{dep}}$ ). The change of peak concentration ranges from  $429.1\%$  to  $-79.1\%$  for the change of deposition rate. Unlike these parameters, the change of peak concentration almost remains constant with the change of longitudinal dispersion coefficient ( $D_L$ ).

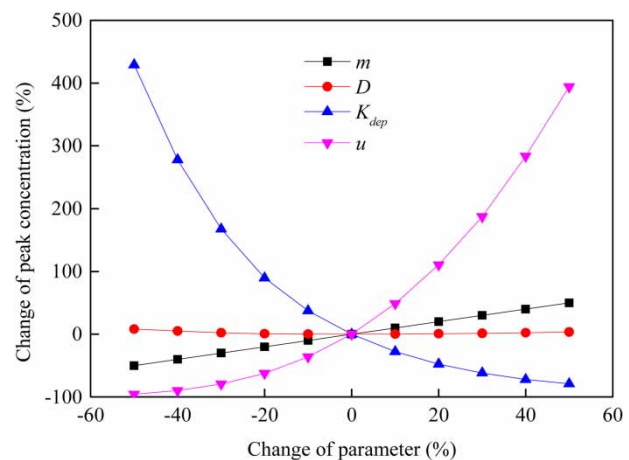


Figure 1 | Relationships between the change of peak concentration and the change of each parameter under pulse injection.

The relationship between particle concentration in the pores ( $C$ ) and the change of each parameter under continuous injection is shown in Figure 2. Under continuous injection, it can be seen that the change of particle concentration increases with the change of injected particle concentration ( $C_0$ ), longitudinal dispersion coefficient ( $D_L$ ) and flow rate ( $u$ ). The change of particle concentration varies from  $-50\%$  to  $50\%$  for the change of injected particle mass,  $-20.6\%$  to  $19.0\%$  for the change of longitudinal dispersion coefficient and  $-98.4\%$  to  $291.2\%$  for the change of flow rate. Meanwhile, the change of particle concentration decreases with the change of deposition rate ( $K_{dep}$ ). The change of particle concentration varies from  $394.7\%$  to  $-78.8\%$  for the change of deposition rate. Similar to the pulse injection,

the particle concentration decreases with the decrease of the flow rate until 0, beyond which it becomes almost constant, while the change of particle concentration increases rapidly as the flow rate increases.

These above behaviors indicate that the deposition rate is negatively correlated with particle concentration. However, the injected particle mass, the injected particle concentration and the flow rate are positively correlated with the particle concentration. The analysis also suggests that the particle concentration is highly sensitive to the flow rate and the deposition rate, while the longitudinal dispersion coefficient effect is negligible.

## MATERIALS AND METHODS

### Set up

In our study, a self-developed sand layer transportation–deposition testing system was used. A schematic diagram of the experimental apparatus is illustrated in Figure 3. All experiments described in this paper were run on this set, which mainly consists of a dynamic system, observation system and data collection system. The studied porous media are placed in a two-dimensional Plexiglas box and the particles are distributed in the water contained in the water tank. The Plexiglas box is sealed with silicon and strong enough to withstand tremendous water pressure. Six connectors are placed on the sides of the box and can be connected with the sensor or pipe. Interior dimensions of the sand box are approximately 1.2 cm (width) by

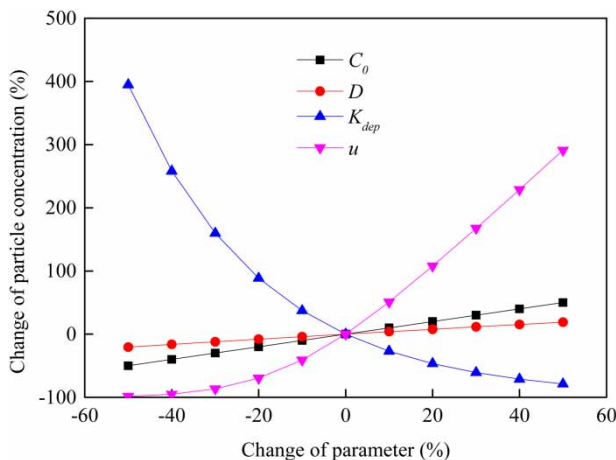


**Figure 2** | Relationships between the change of particle concentration and the change of each parameter under continuous injection.

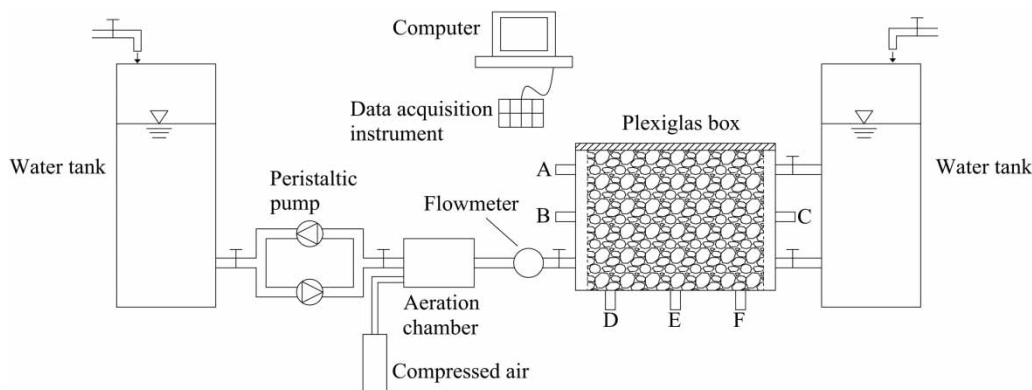


**Figure 3** | Experimental set-up (A–F can be connected to pressure sensor).

50 cm (height) by 60 cm (length parallel to flow). The water in the set was driven by a peristaltic pump and could maintain a constant flow rate. With excellent transparency, transportation and deposition phenomena can be viewed in real time in the Plexiglas box and the sample can be obtained from the outflow pipe.

### Characteristics of the medium and injected particulate matter

The medium used in the study was natural quartz sand and the SiO<sub>2</sub> was not less than 99.6%. The grain size distribution was 15% at 0.18–0.25 mm and 85% at 0.25–0.5 mm.

Red quartz powder was used in the experiments and three size distributions were chosen. Red quartz powder is physically and chemically stable and easy to observe. In addition, its composition is similar to the particles that are clogging in the engineering. The median diameter of particles was chosen as 12.9 μm when we studied the effect of particle concentration. The detailed parameters of sand and quartz powder are shown in Table 1.

### Operating procedure

Generally, the injection mode of particles during column-type tracing experiments involves continuous injection and pulse injection (Tufenkji & Elimelech 2004). In groundwater recharge systems, water source heat pump engineering and pollutant transportation, the concentration of particles is substantially stable. Meanwhile, pulse injection may occur in pollution emergencies, thus continuous injection and pulse injection were both adopted in the study.

To prepare the tests, the quartz sand was washed thoroughly and then packed into the box after being dried for 24 h at 105 °C. The water tank in the upper stream was filled

with particle suspension and the inlet valve was then opened, with flow rate recorded by an electromagnetic flowmeter. The effluent concentrations of suspended particles were measured every 10 seconds in tests, and the transportation and deposition conditions were observed simultaneously.

## RESULTS AND DISCUSSION

### Initial particle concentration

Figure 4 presents the experimental breakthrough curves and corresponding simulated curves for different particle concentrations under two typical ways of injection.

The experimental results show that the sand box was clean in the beginning and the particle concentration started to increase and then reached the peak as particles were transported with the water. The changing trend of particle concentration was different after that, i.e., particle concentration continued to decline under pulse injection and remained stable under continuous injection. All results above-mentioned suggest that particle concentration can influence the transportation and deposition process, and the deposit formations may also vary as the concentration changes.

### Deposition rate coefficient

The deposition rate coefficient ( $K_{dep}$ ) of suspended particles is determined by fitting the experimental breakthrough curves with the theoretical solution of the convection–dispersion equation.

According to classical filtration theory (Tufenkji & Elimelech 2004; Xu *et al.* 2006), the deposition rate coefficient can be expressed as a function with the single-collector

**Table 1** | Physical parameters of quartz sand and quartz powder in experiments

Name	Diameter (μm)	Median diameter (μm)	Density (g/cm <sup>3</sup> )	Porosity (%)	Non-uniform coefficient	Curvature coefficient
Quartz sand	250–500	360	2.65	32	1.3	1.1
Particle 1	5–6.5	5.5	2.65	–	–	–
Particle 2	10–15	12.9	2.65	–	–	–
Particle 3	20–25	22.7	2.65	–	–	–



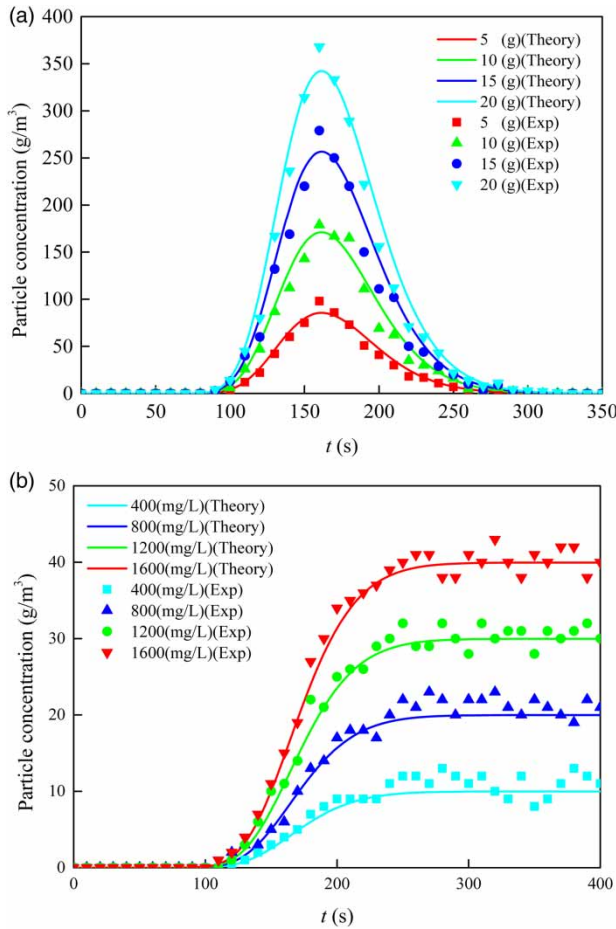


**Figure 4** | Experimental breakthrough curves and corresponding simulated curves for different initial concentrations: (a) pulse injection; (b) continuous injection.

contact efficiency ( $\eta$ ) and the sticking efficiency ( $\alpha$ ), as follows:

$$K_{\text{dep}} = \frac{3(1-\varphi)u}{2d_g} \alpha \eta \quad (9)$$

where  $\varphi$  is porosity,  $u$  is the average flow rate of water in the pores,  $d_g$  is the average grain diameter.

The deposition of particles in porous media results from multi-factors which are dependent upon physical and geometrical parameters. In this study, the chemical mechanisms were neglected from the assessment of the deposition process. Thus particle straining and sedimentation are the principal mechanisms that lead to the deposition of particles, which are closely related to the density and size of suspended particles.

The deposition rate coefficient increases with flow rate and is correlated with the particle size under the seepage

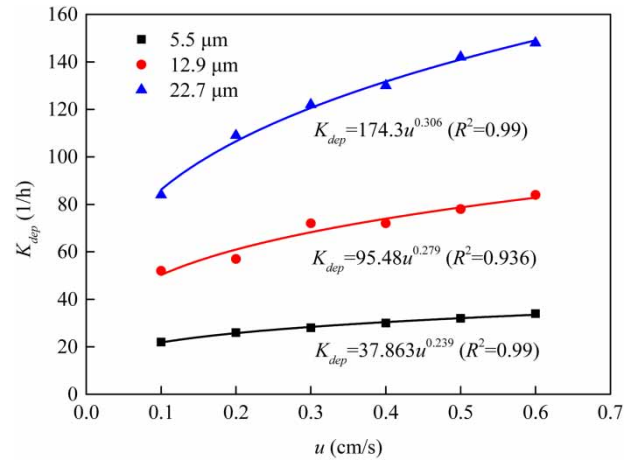


**Figure 5** | Effects of the flow rate and particle size on the deposition rate coefficient.

condition that obeys Darcy's law (Wang *et al.* 2000; Ahfir *et al.* 2009; Kim & Lawler 2012). The relationship between flow rate and deposition rate coefficient is often described with a power law:

$$K_{\text{dep}} = \beta u^n \quad (10)$$

where  $\beta$  and  $n$  are constants that change with particle size.

The various tests carried out under different particle distributions and flow rates indicate that the deposition rate coefficient increases with flow velocity (see Figure 5). These results are in accordance with particle behaviors observed by other researchers (Kim & Lawler 2012).

Figure 5 presents the effects of the flow rate and particle size on deposition rate coefficient. We can observe that  $K_{\text{dep}}$  increases with the size of injected particles at a given velocity. Factors such as constrictions, crevices, and cavities in the sand box are reasons that gave rise to the deposition of particles in porous media. Kretzschmar *et al.* (1997) found a power value of 0.31 for carboxyl latex colloids and 0.18 for humic-coated hematite colloids. For silt particles with large size distribution, the value varies between 0.56 and 0.70 (Wang *et al.* 2000; Ahfir *et al.* 2007, 2009; Kim & Lawler 2012). In the present study, the power value varies from 0.239 to 0.306.

Figure 6 presents the experimental breakthrough curves and corresponding simulated curves for different deposition rate coefficients under two typical ways of injection. As  $K_{\text{dep}}$  changes from 28(1/h) to 122(1/h) under continuous injection, the final value of effluent particle concentration

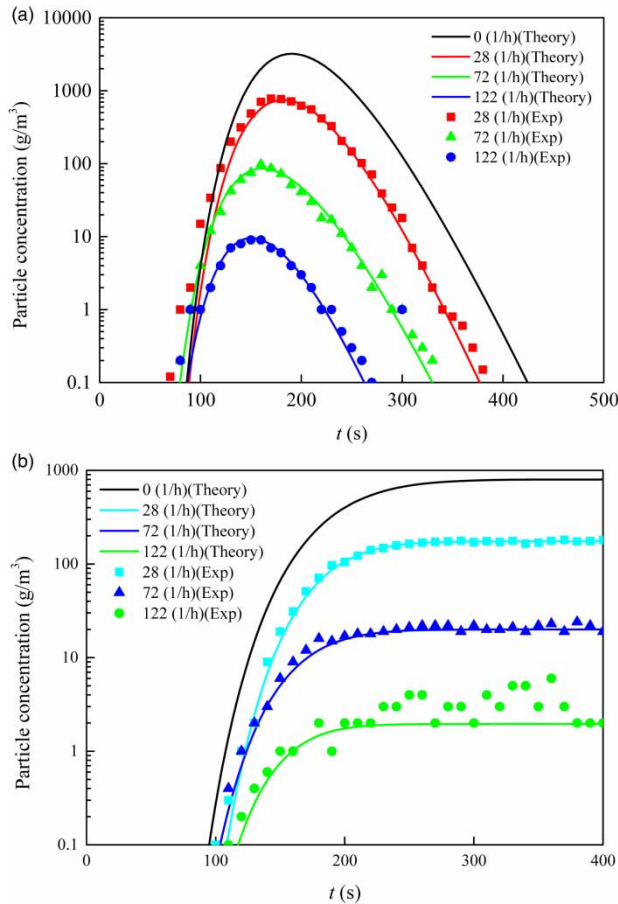


**Figure 6** | Experimental breakthrough curves and corresponding simulated curves for different deposition rate coefficients: (a) pulse injection; (b) continuous injection.

changes from  $2 \text{ g/m}^3$  to  $181 \text{ g/m}^3$ . This indicates that the particle concentration of the effluent is very sensitive to the deposition rate coefficient under both injection modes. For pulse injection, the times needed to reach the peaks of particle concentration of different deposition rate coefficients close to each other. This indicates that the deposition rate coefficient can influence the deposition mass of particles but will not affect their transport velocity markedly.

Different mechanisms of deposition may be the reason for the difference observed in tests. Large particles are dominated by gravity under low flow velocity, thus they can be captured in constricted and cavity sites. As the flow velocity increases, the dominant factor turns into hydrodynamic forces gradually. According to these results, one can deduce that the particle size and flow velocity play important roles in the particle deposition rate coefficient, as well as the process of particle transport and deposition.

### Flow rate and longitudinal dispersion coefficient

The longitudinal dispersion coefficient ( $D_L$ ) is a simplification of hydrodynamic dispersion, in which mechanical dispersion and molecular diffusion are both included. Mechanical dispersion and molecular diffusion are caused by variation in fluid velocity in the pores and the random motion of molecules, respectively.

The longitudinal dispersion coefficient for the average pore velocity is usually expressed with the following equation (Ahfir *et al.* 2009):

$$D_L = \frac{D_0}{\tau^2} + \alpha_L u^n \quad (11)$$

where  $D_0$  is the molecular diffusion coefficient,  $\tau$  is the tortuosity of the porous media,  $\alpha_L$  is the longitudinal dispersivity and  $n$  is an empirical coefficient.

In this study, dispersion is dominated by mechanical dispersion, and molecular diffusion can be neglected, thus Equation (9) can be simplified to

$$D_L = \alpha_L u^n \quad (12)$$

$\alpha_L$  can be expressed as

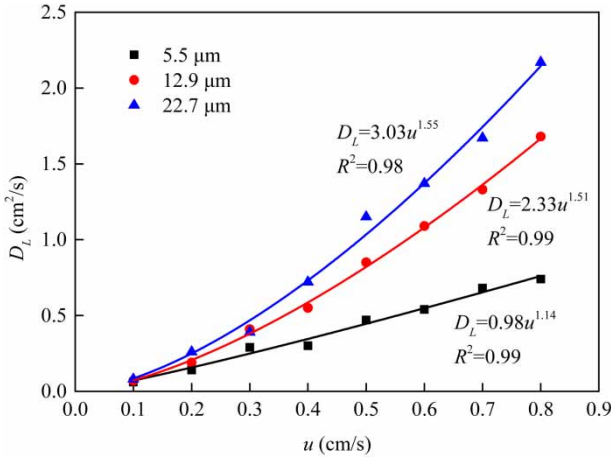
$$\alpha_L = \kappa d_{50}^\beta \quad (13)$$

where  $d_{50}$  is the median particle size,  $\beta$  is a coefficient (approximately 1) and  $\kappa$  is a constant.

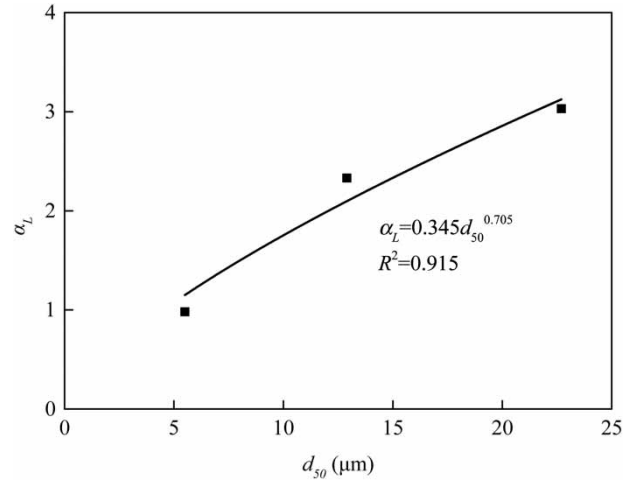
For materials with uniformity coefficient ( $C_u$ ) smaller than 2, the value of the dispersivity is approximately equal to the median grain size (Bernabé *et al.* 2016).

Figure 7 presents the longitudinal dispersion coefficient of suspended particles as a function of the pore water velocity for different particle sizes (i.e., 5.5, 12.9 and  $22.7 \mu\text{m}$ ). The experimental results indicate that the longitudinal dispersion coefficient increases with increasing flow rate. The fitted results show that experimental data satisfy a power law quite well. The results show that the longitudinal dispersion coefficient has an exponent relation to the flow velocity, and the indexes are close to 1. Based on this and considering the difficulty in controlling  $D_L$  in tests, we chose flow velocity to be a substitution parameter for  $D_L$ .

The longitudinal dispersivity may be affected by the materials of the porous media. Ahfir *et al.* (2009) found the



**Figure 7** | Longitudinal dispersion coefficient of different size particles as a function of flow rate.

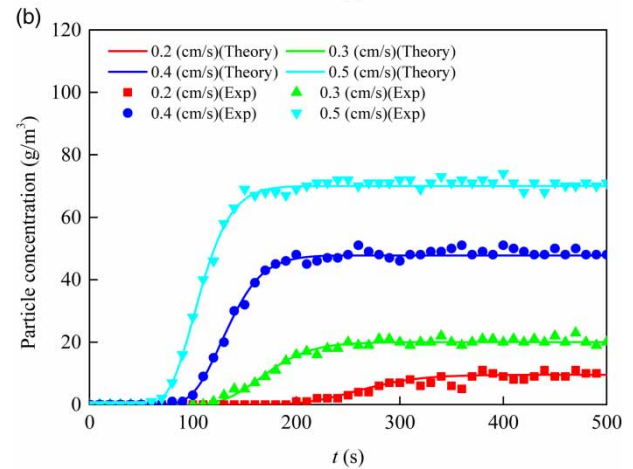
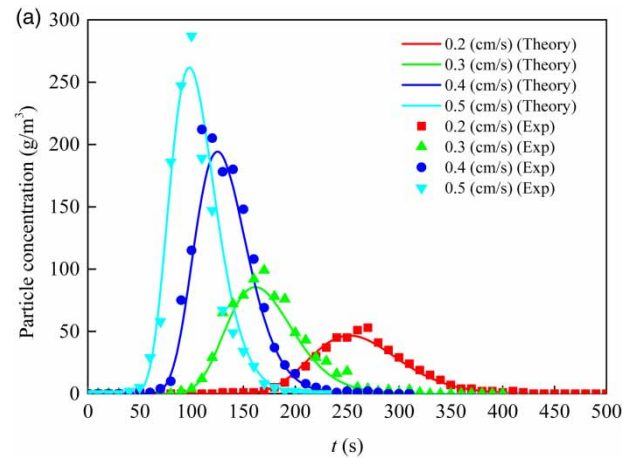


**Figure 9** | Longitudinal dispersivity as a function of the median particle size.

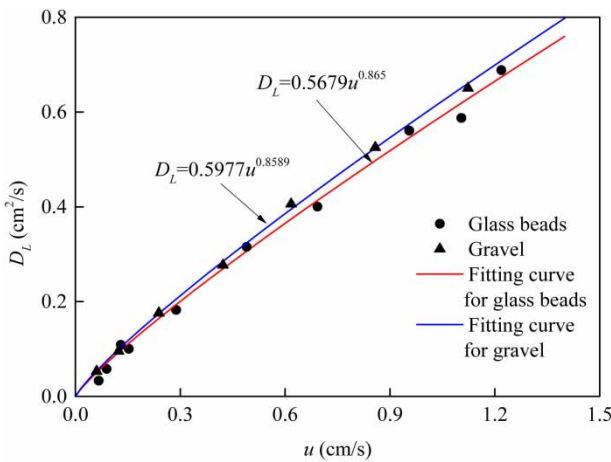
difference of longitudinal dispersivity between glass beads and gravel media through laboratory study, and the results are shown in Figure 8. Due to the broad pore-size distribution, the pore velocity functions are more important. Meanwhile, a uniform pore distribution of glass beads with a single size is also an important factor that led to the difference.

Figure 9 shows the evolution of particle dispersivity in the porous media according to the median particle size (5.5, 12.9 and 22.7 μm). The result indicates that particle dispersivity increases with the suspended particle size and its value varies from 0.98 to 3.03.

Figure 10 presents the observed and theoretical effluent concentration curves with different flow rates under pulse



**Figure 10** | Experimental breakthrough curves and corresponding simulated curves for different flow velocities: (a) pulse injection; (b) continuous injection.



**Figure 8** | Longitudinal dispersion coefficient of suspended particles as a function of flow rate for glass beads and gravel.



injection and continuous injection, respectively. It can be observed that the theoretical result fits the experimental data fairly well. As the flow velocity changes from 0.2 cm/s to 0.5 cm/s under continuous injection, the final value of the effluent particle concentration changes from 10 g/m<sup>3</sup> to 70 g/m<sup>3</sup>, while for pulse injection, the peak value of effluent particle concentration changes from 53 g/m<sup>3</sup> to 287 g/m<sup>3</sup>. This indicates that the particle concentration of the effluent is highly sensitive to the flow rate for both injection modes. We can also get the conclusion that as the flow rate decreases, more particles are deposited in the pores. For both injection modes, there is a big difference between the times required to reach the peak of particle concentration for different flow rates. This indicates that the flow rate can both influence the deposition mass of particles and their transport velocity markedly.

## CONCLUSION

This research was undertaken to study the characteristics of particle transport in saturated porous media. An experimental and analytical investigation is presented, which was aimed at studying the influence of various physical factors on the transport and deposition processes of suspended particles in saturated porous media. The response to pulse and continuous injection provides an effective way of analyzing the process of suspended-particle transport and deposition in porous media.

Results from these experiments show that there exist remarkable differences in transport and deposition characteristics between the two injection modes. For pulse injection, effluent particle concentration has a peak point after injection, and declines rapidly soon after that, while for continuous injection, effluent particle concentration can keep stable after a rising process.

The deposition rate coefficient and longitudinal dispersion coefficient were estimated from the experimental results with the analytical solution of the convection–dispersion model. Sensitivity analysis under the two injection modes indicates that peak concentration and particle concentration are highly sensitive to flow velocity and deposition rate coefficient.

Particle concentration may affect the transport and deposition process in a simple way, i.e., effluent particle

concentration is almost in linear correlation with initial concentration. In contrast, the deposition rate coefficient may affect the transport and deposition process of particles more significantly. The relationship between flow velocity and deposition rate coefficient can be described by a power law, and particle size can also affect the deposition rate markedly. It is worth noting that particle peak concentration and effluent particle concentration change significantly even though there is little change in deposition rate coefficient. The deposition rate coefficient can influence the deposition mass of particles but will not affect their transport velocity markedly. The longitudinal dispersion coefficient has an exponent relation to the flow velocity, and the indexes are close to 1. As flow velocity increases, the particle peak concentration and effluent particle concentration also increase. Meanwhile the time needed to reach this concentration is reduced for both injection modes. Flow rate can influence both the deposition mass of particles and their transport velocity markedly.

From this experimental contribution, it arises that the particle concentration, flow velocity, deposition rate coefficient and longitudinal dispersion coefficient are important factors affecting the transport and deposition process of suspended particles in saturated porous media.

## ACKNOWLEDGEMENTS

This research was supported by the High-level Scientific Research Foundation for the Introduction of Talent, the National Natural Science Foundation of China (Grant No. 41272272) and the National Natural Science Foundation of China (Grant No. 51478368).

## REFERENCES

- Ahfir, N. D., Wang, H. Q., Benamar, A., Alem, A., Massei, N. & Dupont, J.-P. 2007 [Transport and deposition of suspended particles in saturated porous media: hydrodynamic effect](#). *Hydrogeology Journal* **15** (4), 659–668. doi: 10.1007/s10040-006-0131-3.
- Ahfir, N. D., Benamar, A., Alem, A. & Wang, H. Q. 2009 [Influence of internal structure and medium length on transport and deposition of suspended particles: a laboratory study](#).

- Transport in Porous Media* **76** (2), 289–307. doi: 10.1007/s11242-008-9247-3.
- Alvarez, A. C., Hime, G., Marchesin, D. & Bedrikovetsky, P. G. 2007 The inverse problem of determining the filtration function and permeability reduction in flow of water with particles in porous media. *Transport in Porous Media* **70** (1), 43–62. doi: 10.1007/s11242-006-9082-3.
- Bedrikovetsky, P., Siqueira, F. D., Furtado, C. A. & Souza, A. L. S. 2011 Modified particle detachment model for colloidal transport in porous media. *Transport in Porous Media* **86** (2), 353–383. doi: 10.1007/s11242-010-9626-4.
- Bernabé, Y., Wang, Y., Qi, T. & Li, M. 2016 Passive advection-dispersion in networks of pipes: effect of connectivity and relationship to permeability. *Journal of Geophysical Research: Solid Earth* **121** (2), 713–728. doi: 10.1002/2015JB012487.
- Bradford, S. A. & Torkzaban, S. 2013 Colloid interaction energies for physically and chemically heterogeneous porous media. *Langmuir* **29** (11), 3668–3676. doi: 10.1021/la400229f.
- Genuchten, M. T., van Leij, F. J., Skaggs, T. H., Toride, N., Bradford, S. A. & Pontedeiro, E. M. 2013 Exact analytical solutions for contaminant transport in rivers 1. The equilibrium advection-dispersion equation. *Journal of Hydrology and Hydromechanics* **61** (2), 146–160. doi: 10.2478/johh-2013-0020.
- Kasel, D., Bradford, S. A., Šimůnek, J., Heggen, M., Vereecken, E. & Klumpp, E. 2013 Transport and retention of multi-walled carbon nanotubes in saturated porous media: effects of input concentration and grain size. *Water Research* **47** (2), 933–944. doi: 10.1016/j.watres.2012.11.019.
- Kim, J. & Lawler, D. F. 2012 The influence of hydraulic loads on depth filtration. *Water Research* **46** (2), 433–441. doi: 10.1016/j.watres.2011.10.059.
- Kretzschmar, R., Barmettler, K., Grolimund, D., Yan, Y., Borkovec, M. & Sticher, H. 1997 Experimental determination of colloid deposition rates and collision efficiencies in natural porous media. *Water Resources Research* **33** (5), 1129–1137. doi: 10.1029/97WR00298.
- Lanphere, J. D., Rogers, B., Luth, C., Bolster, C. H. & Walker, S. L. 2014 Stability and transport of graphene oxide nanoparticles in groundwater and surface water. *Environmental Engineering Science* **31** (7), 350–359. doi: 10.1089/ees.2013.0392.
- Lee, H., Segets, D., Süß, S., Peukert, W., Chen, S.-C. & Pui, D. Y. H. 2017 Liquid filtration of nanoparticles through track-etched membrane filters under unfavorable and different ionic strength conditions: experiments and modeling. *Journal of Membrane Science* **524**, 682–690. doi: 10.1016/j.memsci.2016.11.023.
- Liu, Q. S., Cui, X. Z., Zhang, C. Y. & Zhan, T. 2014 Effects of particle size on characteristics of transportation and deposition of suspended particles in porous media. *Chinese Journal of Geotechnical Engineering* **36** (10), 1777–1783. doi: 10.11779/CJGE201410003.
- Liu, Q. S., Cui, X. Z., Zhang, C. Y. & Huang, S. B. 2015 Experimental research on release characteristics of deposited particles in porous media. *Chinese Journal of Geotechnical Engineering* **37** (4), 1777–1783. doi: 10.11779/CJGE201504022.
- Ouisse, M., Ichchou, M., Chedly, S. & Collet, M. 2012 On the sensitivity analysis of porous material models. *Journal of Sound and Vibration* **331** (24), 5292–5308. doi: 10.1016/j.jsv.2012.07.018.
- Patel, J., Borgohain, S., Kumar, M., Rangarajan, V., Somasundaran, P. & Sen, R. 2015 Recent developments in microbial enhanced oil recovery. *Renewable and Sustainable Energy Reviews* **52** (C), 1539–1558. doi: 10.1016/j.rser.2015.07.135.
- Pugliese, L., Straface, S., Trujillo, B. M. & Poulsen, T. G. 2015 Relating non-equilibrium solute transport and porous media physical characteristics. *Water, Air, & Soil Pollution* **226** (3), article 59. doi: 10.1007/s11270-015-2353-2.
- Rinck-Pfeiffer, S., Ragusa, S., Sztajn bok, P. & Vandeveld, T. 2000 Interrelationships between biological, chemical, and physical processes as an analog to clogging in aquifer storage and recovery (ASR) wells. *Water Research* **34** (7), 2110–2118. doi: 10.1016/S0043-1354(99)00356-5.
- Sen, T. K. 2011 Processes in pathogenic biocolloidal contaminants transport in saturated and unsaturated porous media: a review. *Water, Air, & Soil Pollution* **216** (1), 239–256. doi: 10.1007/s11270-010-0531-9.
- Tufenkji, N. 2007 Modeling microbial transport in porous media: traditional approaches and recent developments. *Advances in Water Resources* **30** (6–7), 1455–1469. doi: 10.1016/j.advwatres.2006.05.014.
- Tufenkji, N. & Elimelech, M. 2004 Correlation equation for predicting single-collector efficiency in physicochemical filtration in saturated porous media. *Environmental Science & Technology* **38** (2), 529–536. doi: 10.1021/es034049r.
- Wang, H., Lacroix, M., Massei, N. & Dupont, J. P. 2000 Particle transport in a porous medium: determination of hydrodispersive characteristics and deposition rates. *Comptes Rendus de l'Académie des Sciences Series IIA Earth and Planetary Science* **331** (2), 97–104.
- Ward, J. & Dillon, P. 2012 Principles to coordinate managed aquifer recharge with natural resource management policies in Australia. *Hydrogeology Journal* **20** (5), 943–956. doi: 10.1007/s10040-012-0865-z.
- Xu, S., Gao, B. & Saiers, J. E. 2006 Straining of colloidal particles in saturated porous media. *Water Resources Research* **42** (12), 4–20. doi: 10.1029/2006WR004948.
- Yuan, H., You, Z., Shapiro, A. & Bedrikovetsky, P. 2013 Improved population balance model for straining-dominant deep bed filtration using network calculations. *Chemical Engineering Journal* **226** (15), 227–237. doi: 10.1016/j.cej.2013.04.031.